

39. A. Brake and P. Barr, unpublished results.
 40. C. M. Mochle, R. Tizard, S. K. Lemmon, J. Smart, E. W. Jones, *Mol. Cell. Biol.* 7, 4390 (1987).
 41. Abbreviations for the amino acid residues are: A, Ala; C, Cys; D, Asp; E, Glu; F, Phe; G, Gly; H, His; I, Ile; K, Lys; L, Leu; M, Met; N, Asn; P, Pro; Q, Gln; R, Arg; S, Ser; T, Thr; V, Val; W, Trp; and Y, Tyr.
 42. Yeast media and genetic methods are described elsewhere [F. Sherman, G. R. Fink, J. B. Hicks, *Laboratory Course Manual for Methods in Yeast Genetics* (Cold Spring Harbor Laboratory, Cold Spring Harbor, NY, 1986)]. DNA-mediated transformation of yeast spheroplasts was carried out as described [P. M. J. Burgers and K. J. Percival, *Anal. Biochem.* 163,

391 (1987)]. Recombinant DNA methods, with minor modifications, were as described [T. Maniatis, E. F. Fritsch, J. Sambrook, *Molecular Cloning: A Laboratory Manual* (Cold Spring Harbor Laboratory, Cold Spring Harbor, NY, 1982)].

43. Supported in part by a Helen Hay Whitney postdoctoral fellowship and a Lucille P. Markey Biomedical Scholar Award to R.S.F., and by NIH grant GM21841 to J.T. Computer resources were provided by BIONET (NIH grant RR01685). We thank R. Kunisawa for isolation of a *KEX2* cDNA clone and G. Ammerer, P. Barr, G. Payne, and R. Schekman for sharing unpublished information.

24 April 1989; accepted 18 September 1989

Tonotopic Organization of the Auditory Cortex: Pitch Versus Frequency Representation

C. PANTEV, M. HOKE, B. LÜTKENHÖNER, K. LEHNERTZ

According to the place principles of the classical hearing theory, the physical entity frequency is encoded in the auditory periphery as place information (tonotopic representation), which is decoded in more central parts of the auditory system to form the subjective entity pitch. However, this relation is true only for pure-tone signals (spectral pitch); it can be quite different in the case of complex auditory stimuli (virtual pitch), thus requiring a multistage process for pitch formation. Neuromagnetic measurements showed that the tonotopic organization of the primary auditory cortex reflects the pitch rather than the frequency of the stimulus; that is, the pitch formation process must take place in subcortical regions.

THE HISTORY OF HEARING THEORY is determined by two contradictory hypotheses: Helmholtz (1) proposed a systematic spatial representation of pure tones in the auditory system according to their frequency (tonotopic organization), which was subsequently confirmed with invasive physiological methods for any level of the auditory system. Frequency information was assumed to be encoded as place information, and the perceived pitch (place or spectral pitch) was assumed to be related to the place of cortical excitation. However, experiments carried out even before Helmholtz formulated his hearing theory (2) demonstrated that the pitch of complex tones composed of higher harmonics (that is, integral multiples of the fundamental frequency) corresponds to that of a pure tone whose frequency equals that of the fundamental frequency, and that the pitch does not change even when the fundamental frequency (missing fundamental) is removed. The perceived pitch was assumed to be related to the temporal structure of the auditory stimulus (periodicity or virtual pitch). A unification of the two hypotheses—place versus periodicity pitch—was originally attempted by Licklider (3), who

proposed that pure tones are mapped by the auditory system to essentially the same brain structure as are complex tones with similar temporal periods and perceived pitch.

With the advent of biomagnetic measurements, the chance arose to directly test Licklider's unified hypothesis in humans. Auditory-evoked magnetic fields (AEF), because of their great spatial resolution, have already been used to reveal the tonotopic organization of the human primary auditory cortex; that is, neurons are arranged in space according to that frequency to which they respond best (4–6): the depth of the equivalent current dipole (ECD) calculated for wave M100 (termed according to its typical latency of approximately 100 ms) of the AEF increases with the logarithm of stimulus frequency. Using pure-tone and complex-tone stimuli, which are currently known to be the most effective for the perception of periodicity pitch (7, 8), we tested whether the depth of the ECD is the same for a pure-tone stimulus and a complex-tone stimulus producing the same pitch (spectral and virtual, respectively), or whether it moves in the latter case to the place characteristic of the higher harmonics composing the complex-tone stimulus. If the former proves true, then it can be deduced that the "pitch processor," which was postulated by Goldstein (9) and Terhardt

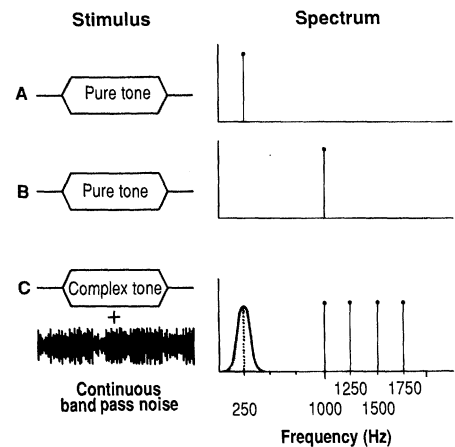


Fig. 1. Scheme of the stimulus conditions in (left) time- and (right) frequency-domain representation. (A) Pure-tone burst of 250 Hz (spectral pitch stimulus); (B) pure-tone burst of 1000 Hz (spectral pitch stimulus); (C) complex-tone burst (virtual pitch stimulus) consisting of the fourth through the seventh harmonic of 250 Hz, presented simultaneously with narrow-band noise centered at 250 Hz.

(10), is located peripheral to the primary auditory cortex.

Three different stimulus signals were used (Fig. 1): bursts (duration, 500 ms) of pure tones, with carrier frequencies of 250 Hz and 1000 Hz, respectively, to elicit a spectral pitch sensation, and bursts of a complex tone composed of the fourth to the seventh harmonic of 250 Hz, which produces a strong virtual pitch. The virtual pitch of the complex-tone signal was tested in 15 individuals and was found to match very well with the spectral pitch of a 250-Hz pure-tone stimulus (250 ± 5 Hz). To ensure that the perceived pitch was not due to combination tones resulting from nonlinear interaction in the auditory periphery, we masked the 250-Hz region of the cochlea by simultaneously presenting a continuous band-pass noise centered at 250 Hz. The intensity of both the stimulus and the masker was 60 decibels (dB) relative to the normal hearing threshold. Three right-handed and three left-handed normal hearing individuals participated in the study. To obtain maximal AEF amplitudes, the measurements were done over the hemisphere contralateral to the side of handedness (11) with contralateral stimulation (5). The magnetic field normal to the skull was measured at 70 positions over the auditory cortex (12) by means of a second-derivative gradiometer, magnetically coupled to a DC-SQUID (superconducting quantum interference device, Biomagnetic Technology). The diameter of the pick-up coil was 20 mm, and the length of the baseline was 50 mm. The output signal of the SQUID control unit was comb filtered, to reduce the noise at the harmonics

Institute of Experimental Audiology, University of Münster, Federal Republic of Germany.

of the power-line frequency, and band-pass filtered from 0.1 Hz (12 dB per octave) to 40 Hz (48 dB per octave). The measurements were carried out in an acoustically and electrically (but not magnetically) shielded room. Instrumental and environmental noise yielded an overall noise level corresponding to about $40 \text{ fT}/\sqrt{\text{Hz}}$. Collection of data consisted in sampling of three subsets of 32 stimulus-related epochs of 1024 ms (sampling rate 250 Hz) for each stimulus condition at each sampling position. Measurements in each subject were distributed at random over different recording sessions; however, within one recording session the sensor was not moved to the next sampling position before the collection of the responses for all stimulus conditions was completed. By this means, variations in the subject's state of vigilance, inhomogeneities of the superimposed magnetoencephalogram (MEG), and geometric (positioning) errors were spread over the different recording positions and thus equally affected the average response to the different stimuli. The parameters (moment, angle, and location in space) of an ECD were calculated for the two major waves of the AEF, M100 and M200, by approximating a theoretical field distribution to the observed one, with a nonlinear least-squares fitting procedure (12).

The ECD depths of waves M100 and M200, the latency values of the two waves, and the goodness of fit is shown in Table 1 for six subjects. The high value of goodness of fit (87% to 96%) indicates the very small residual variance. The most important results are found in the ECD depth of wave

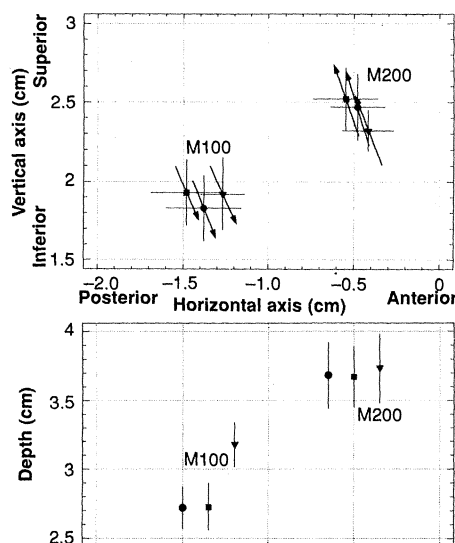


Fig. 2. Mean spatial ECD coordinates of waves M100 and M200 with their standard errors (crossed bars) for the different stimulus signals. The arrows represent amplitude and orientation (with respect to the horizontal axis) of the ECD moment. ●, Virtual pitch (250 Hz); ■, spectral pitch (250 Hz); and ▼, spectral pitch (1000 Hz).

M100. Whereas the depths obtained for the spectral and the virtual pitch signal of 250 Hz do not differ significantly, the difference of the depth of the two to that obtained for the spectral pitch signal of 1000 Hz is significant ($P < 0.05$, Wilcoxon signed-rank test). No significant differences were found for wave M200, nor did the latencies of the two waves differ in the different stimulus conditions.

Mean values of all ECD parameters and their standard errors are summarized for

both waves in Fig. 2. No significant differences were found for any of the remaining ECD parameters for either wave M100 or wave M200 with respect to spectral and virtual pitch. An additional clear-cut result is, however, that the source locations of wave M200 are clearly separated from those of wave M100 ($P < 0.05$), being more anterior (about 9 mm), more superior (about 6 mm), and deeper (about 5 to 10 mm).

Thus it appears that neuromagnetic measurements have allowed the detection of an objective correlate of the purely subjective entity pitch. The results indicate that the spatial arrangement of the generators of the magnetic wave M100 reflects the pitch rather than the spectral contents of the stimulus. This finding suggests the following interpretation: if the perceived pitch of a complex auditory stimulus corresponds to that of a pure tone (missing fundamental) not contained in, and below the bounds of, the frequency spectrum of a complex tone (higher harmonics), then the virtual pitch will determine the place of maximal excitation. This implies that the tonotopic representation at cortex is different from that at the cochlear level, where frequency is the determining parameter, and that the pitch processor must be located peripheral to the generators of wave M100, which are supposed to be in the primary auditory cortex (6).

The fact that the data obtained for wave M200 gave no indication for a tonotopic organization is consistent with the previous tonotopy study of ours (6). The results do not rule out the possibility that the cortical areas responsible for the generation of wave M200 are also tonotopically organized; they may be due to the inadequacy of a single ECD model. However, our findings in neuromagnetic tinnitus studies (13) (in which only the amplitude of the magnetic wave M200 is strongly diminished in tinnitus patients, irrespective of the pitch of tinnitus and of the frequency of the stimulus) seem to support the view that the generators of the magnetic wave M200 are not tonotopically arranged.

Our discovery of a common brain mapping for simple and complex tones provides a new constraint for theories of pitch of complex tones (9, 10, 14–16).

Table 1. ECD depths of waves M100 and M200 for the different stimulus signals (VP, virtual pitch; SP, spectral pitch) as well as wave latencies and goodness of fit (g) for the six subjects (S_1 through S_6).

Subject	M100				M200		
	Conditions	Latencies (ms)	g (%)	Depth (cm)	Latencies (ms)	g (%)	Depth (cm)
S_1	VP (250 Hz)	96	93	3.05	180	94	4.6
	SP (250 Hz)	96	90	3.15	180	96	4.6
	SP (1000 Hz)	100	88	3.55	184	94	4.5
S_2	VP (250 Hz)	92	90	2.1	180	93	2.7
	SP (250 Hz)	92	85	2.0	180	92	2.8
	SP (1000 Hz)	92	88	2.5	176	88	2.7
S_3	VP (250 Hz)	100	92	2.5	176	90	3.2
	SP (250 Hz)	100	91	2.5	176	88	3.4
	SP (1000 Hz)	96	92	3.0	172	87	3.1
S_4	VP (250 Hz)	96	94	2.8	196	90	3.6
	SP (250 Hz)	100	95	2.8	200	92	3.7
	SP (1000 Hz)	96	95	3.2	196	91	3.8
S_5	VP (250 Hz)	100	93	3.15	184	90	4.0
	SP (250 Hz)	100	93	3.25	184	90	3.7
	SP (1000 Hz)	100	95	3.65	184	90	4.1
S_6	VP (250 Hz)	100	92	2.7	188	94	4.0
	SP (250 Hz)	100	91	2.7	184	92	3.8
	SP (1000 Hz)	100	92	3.15	184	94	4.2

REFERENCES AND NOTES

1. H. von Helmholtz, *Die Lehre von den Tonempfindungen als physiologische Grundlage für die Theorie der Musik* (Vieweg, Braunschweig, 1862).
2. A. Secbeck, *Ann. Phys. Chem.* **53**, 417 (1843).
3. J. C. R. Licklider, in *Information Theory*, C. Cherry, Ed. (Butterworths, London, 1956), pp. 253–268.
4. G. L. Romani, S. J. Williamson, L. Kaufman, *Science* **216**, 1339 (1982).
5. C. Elberling, C. Bak, B. Kofoed, J. Lebech, K.

- Saermark, *Scan. Audiol.* **11**, 61 (1982).
6. C. Pantev et al., *Electroencephalogr. Clin. Neurophysiol.* **69**, 160 (1988).
 7. R. J. Ritsma, *J. Acoust. Soc. Am.* **36**, 1191 (1967).
 8. A. J. M. Houtsma and J. L. Goldstein, *ibid.* **51**, 520 (1972).
 9. J. L. Goldstein, *ibid.* **54**, 1496 (1973).
 10. E. Terhardt, *ibid.* **55**, 1061 (1974).
 11. M. Hoke, in *Dynamics of Cognitive and Sensory Processing by the Brain*, E. Basar, Ed. (Springer, Berlin, 1988), pp. 311–318.
 12. C. Pantev, M. Hoke, B. Lütkenhöner, K. Lehnertz, J. Spittka, *Audiology* **25**, 263 (1986).
 13. M. Hoke, H. Feldmann, C. Pantev, B. Lütkenhöner, K. Lehnertz, *Hear. Res.* **37**, 281 (1989).
 14. E. de Boer, in *Handbook of Sensory Physiology*, W. D. Keidel and W. D. Neff, Eds. (Springer, Berlin, 1976), vol. 3, pp. 479–583.
 15. F. L. Wightman, *J. Acoust. Soc. Am.* **54**, 397 (1973).
 16. S. Greenberg, J. T. Marsch, W. S. Brown, J. C. Smith, *Hear. Res.* **25**, 91 (1987).
 17. This work has been supported by grants from the Deutsche Forschungsgemeinschaft. Informed consent was obtained from all subjects before the neuro-magnetic measurements were performed.

31 May 1989; accepted 7 September 1989

Human Chromosome 12 Is Required for Elevated HIV-1 Expression in Human-Hamster Hybrid Cells

CLYDE E. HART,* CHIN-YIH OU, JUDITH C. GALPHIN, JENNIFER MOORE, LEE T. BACHELER, JOHN J. WASMUTH, STEVEN R. PETTEWAY, JR., GERALD SCHOCHETMAN

Host cell factors act together with regulatory genes of the human immunodeficiency virus (HIV) to control virus production. Human-Chinese hamster ovary hybrid cell clones were used to probe for human chromosomes involved in regulating HIV gene expression. DNA transfection experiments showed that 4 of 18 clones had high levels of HIV gene expression measured by both extracellular virus production and trans-activation of the HIV long terminal repeat in the presence of the trans-activator (*tat*) gene. Karyotype analyses revealed a 94% concordance (17/18) between human chromosome 12 and HIV gene expression. Other chromosomes had an 11 to 72% concordance with virus production.

THE AMOUNT OF TRANSCRIPTION and virus production of human immunodeficiency virus type 1 (HIV-1) is controlled by trans-acting regulatory genes encoded in the viral genome (1) and by agents known to activate T cells (2). Cellular factors are involved in mediating the response to both the trans-activating genes (3–5) and T cell activators (4, 6–8). The trans-activator response element (TAR) of the viral long terminal repeat (LTR) is required for *tat*-induced trans-activation of the LTR (9). *Tat* has not been shown to bind directly to TAR, suggesting that cellular factors are involved. Cellular proteins can bind to TAR in the absence of the *tat* protein (3, 10). The relation between these DNA binding proteins associated with TAR and the regulation of *tat*-directed trans-activation is not known.

We wished to identify the human chro-

mosomes that encode cellular factors, which, in the presence of *tat*, support enhanced HIV gene expression. A series of human-Chinese hamster ovary (CHO) hybrid cell clones that contain defined sets of human chromosomes were assayed for production of extracellular HIV and for *tat*-induced trans-activation of the LTR. The results indicate that the presence of both human chromosome 12 and the HIV *tat* gene was necessary for high levels of viral gene expression in the human-hamster hybrid cells.

The ability of the hybrid clones to produce extracellular virus was tested by transfection with an infectious molecular clone of HIV DNA, pZ6neo (11) (Fig. 1). The parent CHO cell line and 12 of 18 hybrid clones transfected with pZ6neo DNA did not produce detectable levels of virus 3 or 6 days after transfection. Clones 151, 271, 863, and 907 produced significant amounts of extracellular virus on day 3 and more on day 6 (Fig. 1). The amount of HIV antigen produced from the human RD cell line (20-fold above cutoff; day 6), the positive control for virus production, was always greater than that of the human-hamster hybrid clones (3.4- to 5.9-fold above cutoff; day 6). Although two hybrid clones, 488 and 671, produced some detectable extracellular virus

on day 6, the amount was much lower than that in the other four virus-positive clones. Intracellular viral p24 was assayed to identify any hybrid clone that synthesized viral proteins but did not assemble and export the virus. Intracellular viral p24 levels, however, did correlate to extracellular particle-associated p24 (12) indicating that the rate-limiting step in virus production occurred before viral protein synthesis. Cell growth rates (12), DNA uptake, and the ability of the cells to express transfected DNA (Table 1) did not correlate to HIV production.

Hybrid clones with enhanced virus production (clones 151, 271, 863, and 907) were at least 28% discordant with all human chromosomes except for chromosome 12, which was 6% (1 of 18) discordant (Table 1). Without human chromosome 12, hybrid clones could not support enhanced virus production, which indicated that genes encoded on this chromosome were involved in the increase of HIV gene expression. Hybrid clones 151, 271, 863, and 907 contained chromosome 12 in at least 80% of the cells tested at three separate karyotype analyses (see Table 1). Hybrid clone 864, which contained chromosome 12 but was negative for virus production (Fig. 1 and Table 1), had a continually decreasing percentage of cells containing chromosome 12 (70 to 0%). Because hybrid clones containing chromosomes 7, 10, and 16 could not be used for concordance analysis (see Table 1), additional experiments are necessary to determine their possible role in HIV gene expression.

Because the gene for the CD4 cell surface receptor of HIV (13) is encoded on chromosome 12 (14), the hybrid clones were assayed for cell surface CD4 molecules, which could amplify a basal level of HIV production by reinfection. Cell surface CD4, detected by immunostaining and flow cytometry (15), was present on only one of the four hybrid clones (907), which produced a high level of virus (12); clones 151, 271, 863, and RD cells, which produced HIV at a level greater than or equal to clone 907, were CD4-negative. Mouse L cells, stably transfected with human CD4 DNA, will bind HIV but are not permissive to HIV infection (16), further indicating that cell surface CD4 expression is not sufficient for supporting HIV infection. These results suggest that cellular factors encoded on chromosome 12, other than the CD4 molecule, were responsible for the increased HIV gene expression.

Because the presence of a functioning *tat* gene is required for enhanced viral gene expression (17), the hybrid clones and CHO cells were tested for their ability to support *tat* trans-activation of the LTR (Fig. 2).

C. E. Hart, C.-Y. Ou, J. C. Galphin, J. Moore, G. Schochetman, Centers for Disease Control, Atlanta, GA 30333.

L. T. Bacheler and S. R. Petteway, Jr., Medical Products Department, E. I. du Pont de Nemours, Wilmington, DE 19898.

J. J. Wasmuth, University of California School of Medicine, Irvine, CA 92717.

*To whom correspondence should be addressed at the AIDS Program, Mailstop D12. Current address: Smith, Kline and French Laboratories, King of Prussia, PA 19406.